



**HAL**  
open science

## Scalar current limit from the beta-neutrino correlation: the WISArD experiment

V. Araujo-Escalona, P. Alfaut, P. Ascher, D. Atanasov, B. Blank, L. Daudin,  
X. Fléchar, M. Gerbaux, J. Giovanazzo, S. Grévy, et al.

### ► To cite this version:

V. Araujo-Escalona, P. Alfaut, P. Ascher, D. Atanasov, B. Blank, et al.. Scalar current limit from the beta-neutrino correlation: the WISArD experiment. 42nd Symposium on Nuclear Physics, Jan 2019, Cocoyoc, Mexico. pp.012003, 10.1088/1742-6596/1308/1/012003 . hal-02327692

**HAL Id: hal-02327692**

**<https://hal.science/hal-02327692v1>**

Submitted on 9 Nov 2020

**HAL** is a multi-disciplinary open access archive for the deposit and dissemination of scientific research documents, whether they are published or not. The documents may come from teaching and research institutions in France or abroad, or from public or private research centers.

L'archive ouverte pluridisciplinaire **HAL**, est destinée au dépôt et à la diffusion de documents scientifiques de niveau recherche, publiés ou non, émanant des établissements d'enseignement et de recherche français ou étrangers, des laboratoires publics ou privés.

PAPER • OPEN ACCESS

## Scalar current limit from the beta-neutrino correlation: the WISArD experiment

To cite this article: V. Araujo-Escalona *et al* 2019 *J. Phys.: Conf. Ser.* **1308** 012003

View the [article online](#) for updates and enhancements.

### Recent citations

- [Decay microscope for trapped neon isotopes](#)  
Ben Ohayon *et al*



**IOP | ebooks™**

Bringing together innovative digital publishing with leading authors from the global scientific community.

Start exploring the collection—download the first chapter of every title for free.

# Scalar current limit from the beta-neutrino correlation: the WISArD experiment

V. Araujo-Escalona<sup>1</sup>, P. Alfaut<sup>2</sup>, P. Ascher<sup>2</sup>, D. Atanasov<sup>1,3</sup>, B. Blank<sup>2</sup>, L. Daudin<sup>2</sup>, X. Fléchar<sup>4</sup>, M. Gerbaux<sup>2</sup>, J. Giovinazzo<sup>2</sup>, S. Grévy<sup>2</sup>, T. Kurtukian Nieto<sup>2</sup>, E. Liénard<sup>4</sup>, L. Nies<sup>5</sup>, G. Quémener<sup>4</sup>, M. Roche<sup>2</sup>, N. Severijns<sup>1</sup>, S. Vanlangendonck<sup>1</sup>, M. Versteegen<sup>2</sup>, P. Wagenknecht<sup>1</sup>, D. Zakoucky<sup>6</sup>.

<sup>1</sup> KU Leuven, Department of Physics and Astronomy, Instituut voor Kern- en Stralingsfysica, Celestijnenlaan 200 D, B-3001 Leuven, Belgium.

<sup>2</sup> CEN Bordeaux-Gradignan, 19 Chemin du Solarium, CS 10120, F-33175 Gradignan, France.

<sup>3</sup> CERN, CH-1211 Genève 23, Switzerland.

<sup>4</sup> LPC Caen, ENSICAEN, Université de Caen, CNRS/IN2P3, Caen, France.

<sup>5</sup> II. Physics Institute, University of Giessen, Germany.

<sup>6</sup> Nuclear Physics Institute CAS, Řež, Czech Republic.

E-mail: victoria.araujoescalona@kuleuven.be

**Abstract.** Beta - neutrino correlation measurements are key in the research of physics beyond the Standard Model. In pure Fermi beta transitions, the beta-neutrino correlation coefficient,  $a_{\beta\nu}$ , is sensitive to the presence of scalar currents. The present limits were established by experimental studies of various nuclear systems with allowed Fermi transitions. A new experiment to improve the constraints on scalar currents is being developed, by the WISArD collaboration at ISOLDE/CERN, where the aim is to measure the energy shift of the  $\beta$ -delayed protons emitted from the isobaric analogue state of the  $^{32}\text{Ar}$  ground state. To enhance the sensitivity, protons and positrons are guided by a strong magnetic field and measured in coincidence between the two detection configurations located on both sides of a catcher foil in which the radioactive samples are implanted. Kinematic energy shifts of the protons in coincidence with positrons, in the same or opposite hemisphere of the catcher foil, will be more or less pronounced as a function of the possible scalar current component of the weak interaction. Details of the apparatus and preliminary results of the experiment are presented.

## 1. Introduction

The Vector – Axial – vector (V-A) formalism [1] of nuclear  $\beta$  decay has been established a few decades ago and ever since has been continuously tested in an effort to find physics beyond the Standard Model (SM). There are two main experimental approaches to test the formalism: one is to perform collider experiments [2, 3] at very high energies to find evidence of new particles, another one uses low-energy  $\beta$ -decay experiments to determine different aspects of the interaction [4]. The latter approach is a primary method of new experiments that provide high precision tests of the discrete symmetries in the SM, and search for non-SM interaction components. Experimental error bars still leave sufficient room for the possible existence of other types of weak interaction in  $\beta$  decay, i.e. scalar (S), tensor (T), and pseudoscalar (P) type interactions. Together with the well-known vector (V) and axial -vector (A) interactions, they



appear in the most general form of the  $\beta$  decay Hamiltonian at the present level of precision. The P interaction can be neglected in the non-relativistic description of nucleons [5]. The coupling constants  $C_i$  and  $C'_i$  ( $i = S, V, A$  and  $T$ ) for the different types of weak interaction have to be determined experimentally.

## 2. Weak interaction studies with radioactive samples

The experimental determination of the magnitude of the coupling constants ( $C_i$  and  $C'_i$ ) for a given exotic current is well described by Jackson et al. [6] by using the decay rate distribution. Following their formalism, the decay rate is given as a function of the total energies and momenta of the particles of the decaying system, including their spins. For example, the angular and energy distributions of the electron and neutrino in the case of a decay of unpolarized nuclei or neutrons will have the form

$$\omega(E_e) = \omega_o(E_e)\xi\left(1 + \frac{\vec{p}_e \cdot \vec{p}_\nu}{E_e E_\nu}a + \frac{m_e}{E_e}b + \dots\right) \quad (1)$$

where the function  $\omega_o(E_e)$  represents the phase space factor and the Fermi function,  $m_e$  is the rest mass of the electron and  $E_e$  is the total energy of the  $\beta$  particle. The coefficients  $a$  ( $\beta - \nu$  angular correlation) and  $b$  (Fierz interference term) are called correlation coefficients. Each coefficient measurement contains specific information on the dynamics of the decay, expressed in terms of Fermi (F) and Gamow-Teller (GT) nuclear matrix elements,  $M_F$  and  $M_{GT}$  respectively, and the coupling constants  $C_i$  and  $C'_i$ , with  $\xi$  defined as

$$\xi = |M_F|^2 (|C_S|^2 + |C_V|^2 + |C'_S|^2 + |C'_V|^2) + |M_{GT}|^2 (|C_T|^2 + |C_A|^2 + |C'_T|^2 + |C'_A|^2) \quad (2)$$

This work is concentrating on the search of scalar currents. It requires the determination of the  $\beta - \nu$  correlation coefficient,  $a_{\beta\nu}$ , and the Fierz interference term in Eq. (1). The latter parameter cannot be neglected when measuring the  $\beta - \nu$  angular correlation coefficient, since it does not depend on any particular spin or momentum vector. Thus, it is more convenient to define a parameter  $\tilde{a}$

$$\tilde{a} = \frac{a}{1 + b'} \quad (3)$$

where  $b' \equiv \langle m/E_e \rangle b$  and  $\langle \rangle$  stands for the weighted average over the observed part of the  $\beta$  spectrum [5]. However, within the SM, with only V and A interactions present, the Fierz interference term is equal to zero, such that  $\tilde{a} \equiv a$ . Then the  $a_{\beta\nu}$  parameter can be expressed in terms of the Fermi and Gamow-Teller matrix elements:

$$a\xi = |M_F|^2 \left[ -|C_S|^2 + |C_V|^2 - |C'_S|^2 + |C'_V|^2 \right] + \frac{|M_{GT}|^2}{3} \left[ |C_T|^2 - |C_A|^2 + |C'_T|^2 - |C'_A|^2 \right] \quad (4)$$

Equation (4) highlights the sensitivity of the  $a_{\beta\nu}$  parameter to possible scalar and tensor contributions, making it an interesting observable in the search for physics beyond the SM. This parameter depends quadratically on the coupling constants and thus, in order to get a high accuracy measurement and constrain its value, higher experimental precision is required.

If the decay rate can be measured as a function of the angle of emission between beta and neutrino, the correlation coefficients  $a_{\beta\nu}$  and  $b$  can be constrained and a limit can be found on the relevant coupling constants. From Eq. (4) it becomes clear that the scalar and tensor interactions can be determined independently, i.e. by studying pure Fermi- and GT- transitions,

given as result Eq. (5) and Eq. (6), respectively. Indeed, T and V make the largest  $a_{\beta\nu}$  value when beta and neutrino are emitted in the same direction and hence result in a higher probability of small emission angles. On the other hand, S and A have the opposite effect. They reduce the  $a_{\beta\nu}$  value and thus favour emission of beta and neutrino in opposite direction.

$$a_F \simeq 1 - \frac{|C_S|^2 + |C'_S|^2}{|C_V|^2} \quad (5)$$

$$a_{GT} \simeq -\frac{1}{3} \left[ 1 - \frac{|C_T|^2 + |C'_T|^2}{|C_A|^2} \right] \quad (6)$$

If one considers only SM contribution the previous parameters reduce to  $a_F = 1$  and  $a_{GT} = -\frac{1}{3}$ . It is important to note here that the SM is actually quite good at describing the weak interaction. The current limits on the norm of the scalar coupling constant are  $|C_S/C_V| = 0.0014(12)$  for left-handed currents and  $|C_S/C_V| < 0.068$  (95% C.L.) for right-handed currents [5]. In order to improve this value, new measurements of the  $a_{\beta\nu}$  parameter have to reach the  $10^{-3}$  level of precision.

### 2.1. Motivation

A straightforward way to obtain experimental information about the  $a_{\beta\nu}$  parameter would be to measure the correlation between the leptons emitted in the decay i.e. the  $\beta$  particle and the neutrino. Since a direct measurement of the neutrino is almost impossible, a common way to infer the  $a_{\beta\nu}$  parameter is by performing high precision measurements of the recoiling daughter nuclei. However, this is also a difficult task, since the energy of the recoil is only a few hundred eV. In spite of that there is another insightful way to have information on  $a_{\beta\nu}$ ; the beta-delayed proton emission. This requires using nuclei that are subject to  $\beta$  decay transitions and decay into the Isobaric Analogue State, *IAS*. An IAS is one that has a similar structure to the original decaying state allowing measurements between the  $\beta$  particle coming from the original decay and the emitted particle coming from the IAS state of the daughter nuclei. This technique was used by Schardt et al. [8] as a first observation of the  $\beta - \nu$  recoil broadening for  $\beta$  delayed protons in  $^{32}\text{Ar}$  and  $^{33}\text{Ar}$  decay. This experiment was later improved by Adelberger et al. [7]. The most precise experiments performing measurements in the  $a_{\beta\nu}$  parameter in search currents are presented in Table 1.

Table 1: Experimentally determined values for the  $a_{\beta\nu}$  correlation coefficient for scalar contributions.

Isotope	$a_{\beta\nu}$	Technique	Reference
$^{32}\text{Ar}$	0.9989(52)	$\beta^+$ delayed $p$ broadening	Adelberger et al. 1999 [7]
$^{32}\text{Ar}$	1.0050(52)*	$^{32}\text{Ar}$ mass measurements	Blaum et al. 2003 [9]
$^{38}\text{K}^m$	0.9981(30)	$\beta^+$ delayed $\gamma$ shift	Gorelov et al. 2005 [10]

\* Using the exact measure of the  $^{32}\text{Ar}$  mass, the previous  $a_{\beta\nu}$  value obtained by Adelberger et al. was updated.

The values presented in Table 1 are in agreement with the expected value from the SM,  $a_F = 1$ , but the error bars still leave sufficient room for the possible existence of exotic currents.

The **WISArD** (**Weak Interaction Studies with  $^{32}\text{Argon Decay}$** ) experiment aims at a precise measurement of the  $a_{\beta\nu}$  parameter using for the first time the kinematic energy shift of the  $\beta$  delayed protons emitted from the IAS of the  $^{32}\text{Ar}$  ground state. Note that the measurements performed in the past by Schardt et. al. [8] and Adelberger et. al. [7], determined the broadening of these  $\beta$  delayed protons using the  $^{32}\text{Ar}$  nuclide.

### 2.2. Experimental technique: The 0.1% challenge

The following section describes the proof-of-principle experiment carried out in the fall of 2018. We have decided to use radioactive argon isotope as our case of study due to the fact that the final state of the superallowed Fermi transition, the IAS in  $^{32}\text{Cl}$ , is unbound to proton emission. A schematic diagram of this process is shown in Figure 1.

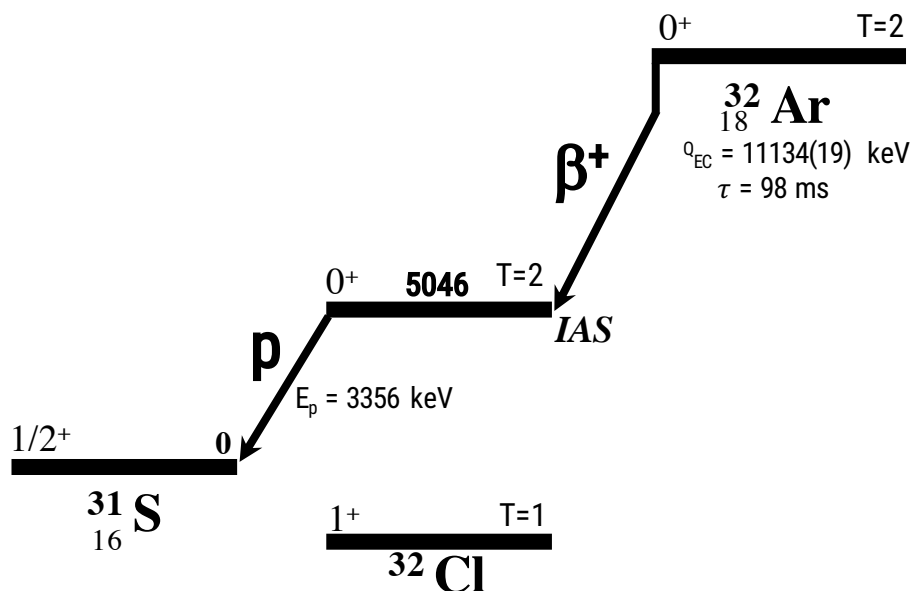


Figure 1: Schematic of the  $\beta$ -delayed proton decay of  $^{32}\text{Ar}$  via the IAS.

Monte Carlo ( $MC$ ) simulations were performed initially to test the feasibility of the experiment (see Figure 2) [12]. The simulated energy spectrum presents two cases for the protons emitted from the IAS in  $^{32}\text{Cl}$ : (left) the dominant vector and (right) the exotic scalar contribution of the weak interaction. As one can see, there is a clear difference between the two currents. The vector current induces a kinematic shift on the proton energies (left side in Figure 2), whereas for a scalar current there is basically no difference with respect to the hemispheres in which the proton and positron are detected (right side in Figure 2).

This emphasizes that the energy resolution in the proton detectors will be crucial. If a proton resolution below 10 keV can be reached, a new limit for  $a_{\beta\nu}$  of the order of 0.1% is reachable.

Due to the recoil the daughter nucleus gets from the emission of the positron and the neutrino, the proton is emitted from a moving source and is subject to a kinematic shift. If the proton is emitted in the direction in which the daughter nucleus moves it gets a boost in energy, (green and blue in Figure 2), whereas it is slowed down if emitted in opposite direction (red and pink, in Figure 2). Whatever is the case, measurements of the kinematic shift in the proton's energy is much easier to measure with high precision than a broadening. Keeping in mind that the correlation coefficient is sensitive to the energy and angle of the beta particle, we decided to measure positron-proton coincidences. Therefore, the detection setup requires a strong magnetic field to guide the positrons away from the proton detectors, reducing the background in the proton energy spectrum.

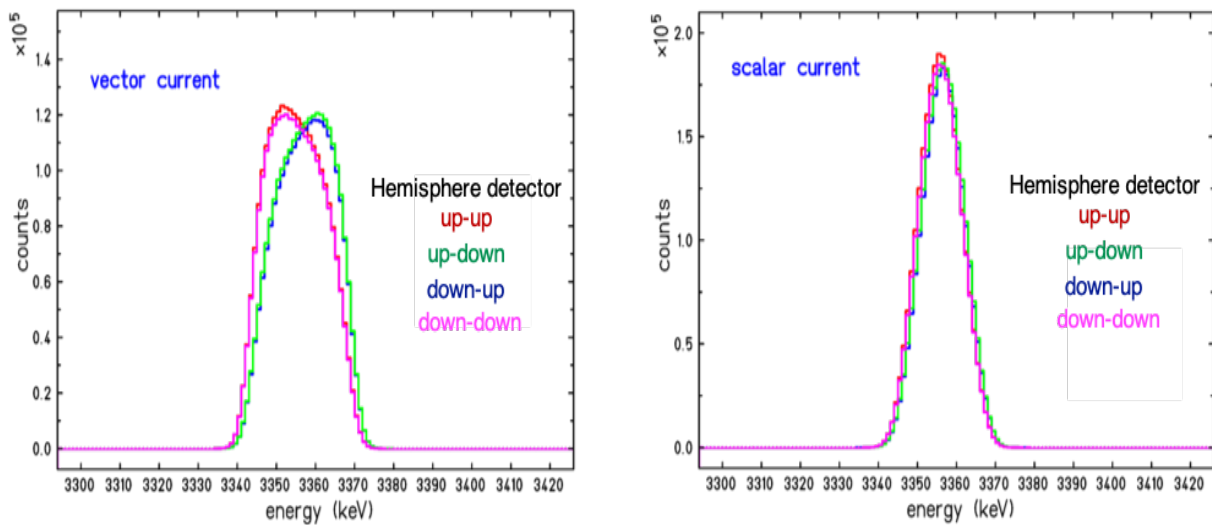


Figure 2: MC simulations showing the observed proton energy histogram from a pure vector and a pure scalar decay. The vector current induces a kinematic shift on the proton energies, whereas for a scalar current there is basically no difference with respect to the hemispheres in which the proton and the positron are detected.

### 3. WISArD setup

The new WISArD experiment reutilises the former WITCH superconducting magnet situated in the ISOLDE Hall at CERN. For this experiment a 1.4 GeV proton beam impinged on a thick CaO target. From the produced radioactive elements, the High Resolution Separator (HRS) selects the  $^{32}\text{Ar}$  ions which are then send through REXtrap. From here, the continuous  $^{32}\text{Ar}$  beam with an estimated intensity of the order of 2000 ions/s, got injected in the WISArD setup. After the beam traversed the horizontal beamline, the 30 keV  $^{32}\text{Ar}$  beam is steered into the 7m high vertical beamline, where it is transported to the catcher foil situated at the geometrical center of a strong magnetic field (4T) generated by the superconducting magnet. The experimental setup is presented schematically in Figure 3. It shows how the  $^{32}\text{Ar}$  beam is implanted continuously on a  $6\mu\text{m}$  thick Mylar foil where the decay takes place. The protons emitted from the  $\beta$  delayed decay, slightly affected by the strong magnetic field, were detected on either side of the catcher foil using a mirrored configuration of an assembly of four silicon detectors. Positrons were guided by the magnetic field lines to a plastic scintillator mounted on the up plate downstream the mylar foil. Due to their bending radius, they cannot reach the proton detectors. In the first online proof-of-principle experiment, only one  $\beta$  detector was used. A second  $\beta$  detector located on the lower plate, upstream the mylar foil, is contemplated for future measurements.

The new detection system was expected to have a good energy resolution due to the low temperature inside the superconducting magnet. The signals were amplified by pre-amplifiers, which are located inside the superconducting magnet and developed to work under vacuum condition and strong magnetic fields, then digitized and recorded by the FASTER [13] data-acquisition system, which uses the ROOT Histogram Builder, *RHB*, for online visualization and data analysis. ROOT-trees contain single proton energy histograms and coincidence events between silicon and scintillator detectors. Data taken over a period of 20 hours using a 4T magnetic field are presented in the following section.

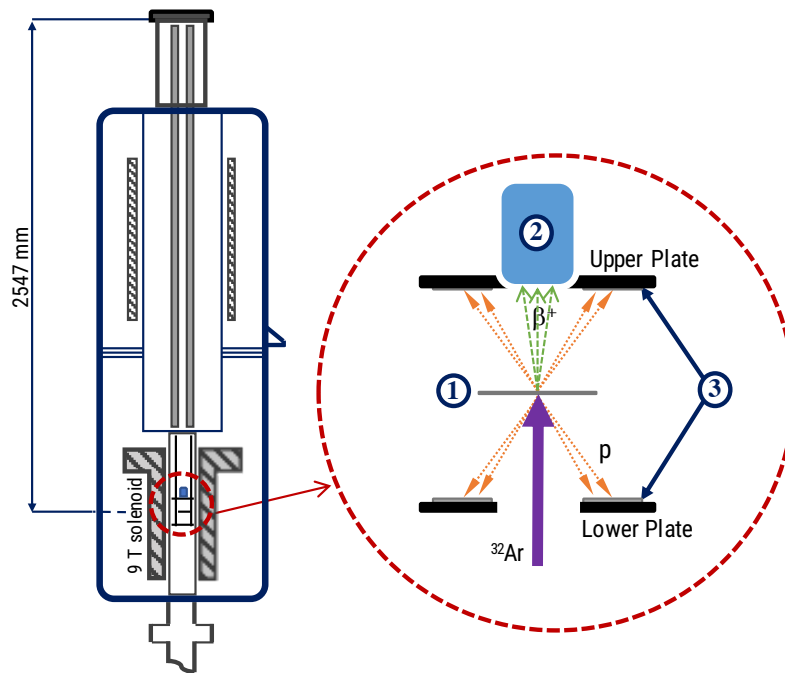


Figure 3: Schematic view of the WISArD magnet and detection setup. Left: the superconducting magnet of the former WITCH experiment in its cryostat. Notice the distance between the geometrical center of the detection setup (same as the geometrical center of the 9T solenoid), and the top flange, the latter being the only access to the system. Right: close-up of the detection setup in the center of the magnet. The 30 keV  $^{32}\text{Ar}$  beam (purple arrow) is implanted in the mylar foil (1) where the decay takes place. Beta particles are guided by 4T magnetic field lines to the plastic scintillator (2) (Polystyrene) on the up plate. The Upper and Lower aluminium plates of 125 mm diameter and with a 20 mm hole in the center at both sides of the mylar foil are distance of 70 mm from the foil. Protons are detected with two disks of four round silicon detectors (3), 30 mm diameter each, fixed on these plates are installed. For the proof-of-principle experiment, only one  $\beta$  detector was installed.

#### 4. Preliminary results

Preliminary results obtained from the campaign in November 2018 are presented.

When both leptons (i.e. positron and neutrino) emitted from the super-allowed Fermi  $\beta^+$  decay, go in the same hemisphere, considering the mylar foil as a reference, they give to the recoiling nuclei a boost in energy. Following this approach, the kinematic energy shift will be more or less pronounced according to the direction of the emitted protons. Given that protons are emitted in any direction and are sensitive to the kinematic energy shift, we need to distinguish between the two directions of the recoiling daughter nuclei (i.e. the  $^{32}\text{Cl}$ ).

In order to evaluate the energy shift of the detected protons, we consider the data for one silicon detector in the upper and lower hemisphere. In the analysis hereafter we are considering only the protons emitted from the IAS at  $E_{lab} = 3356(2)\text{keV}$ . The single histogram was fitted with a Gaussian in the Fermi energy region. In Figure 4a, the Region Of Interest (ROI) in the Fermi energy peak is shown in with their close-up shown in 4b. The Fermi energy peak is expected at  $E_F = 3264.92(26)\text{keV}$  due to the energy loss in the mylar foil.

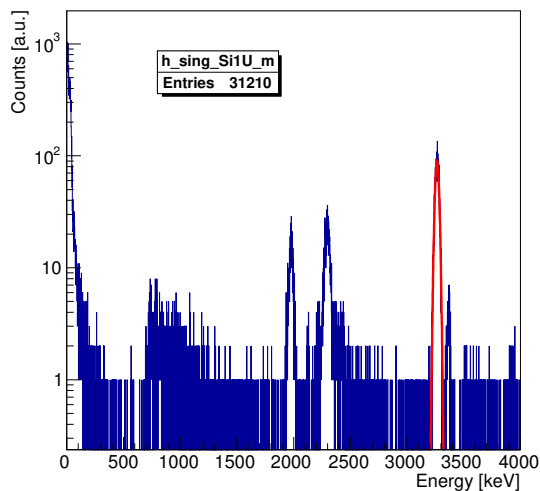
Figure 4c shows the protons that travel in the same the direction as the emitted  $\beta$  particles, (i.e. coincidence- histogram). Currently, the beta detector is located downstream the  $^{32}\text{Ar}$  beam



(upper plate) allowing us to make coincidences between the  $\beta$  particles measured in the upper plate, (i) protons going to the upper plate, and (ii) protons going to the lower plate (opposite direction as the  $\beta$  emitted). The first case is presented in Figure 4c. In figure 4d, the close-up into the ROI Fermi energy peak is presented and fitted with a Gaussian yielding a mean energy value of  $E = 3259.95(36)$  keV.

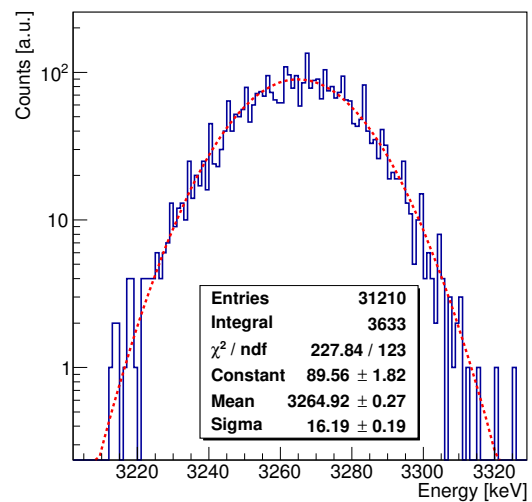
The proton energy difference between the histograms in Figures 4b and 4d (i.e., single and coincidences in the upper hemisphere) is around 5 keV in the mean energy value. Expected reduction in the proton energy showed by the MC simulations (red in Figure 2).

**Proton Energy Peak (UPPER PLATE)**



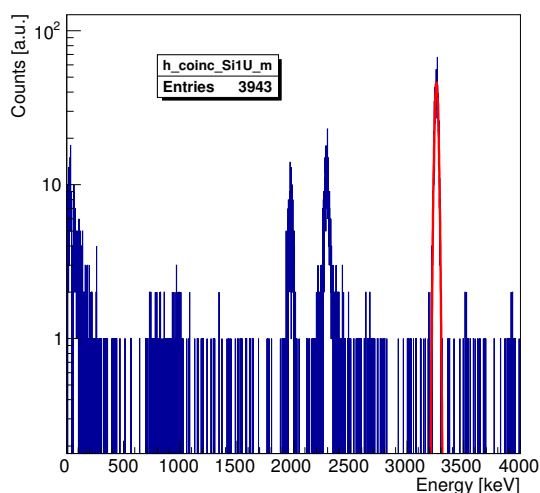
(4a) Proton energy spectrum fitted in the expected ROI (Fermi peak)

**Close-up Proton Energy Peak (UPPER PLATE)**



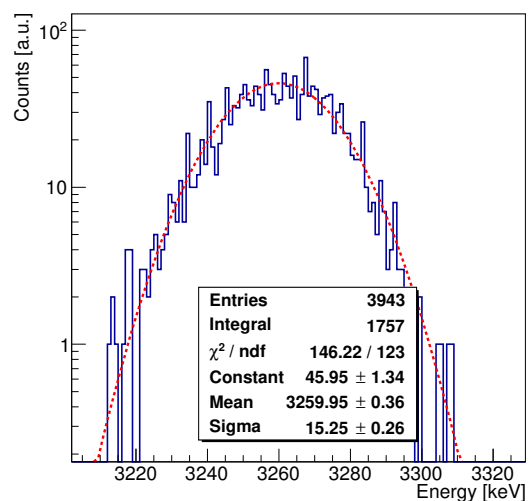
(4b) Close-up to the fit in (4a) yielding a mean value of  $E = 3264.92(26)$  keV

**p-beta coincidence (UPPER PLATE)**



(4c) p-beta coincidence energy spectrum fitted in the expected ROI (Fermi peak)

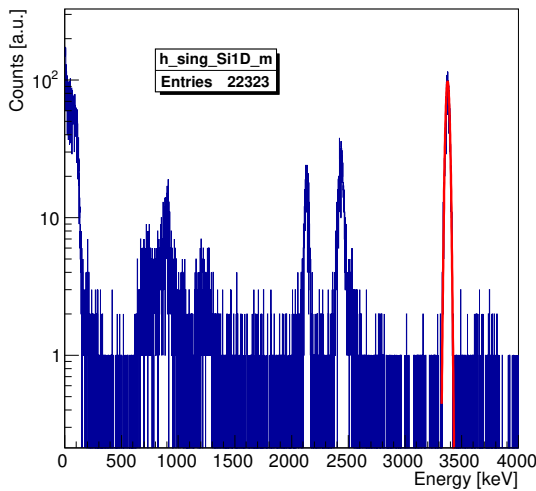
**Close-up p-beta coincidence (UPPER PLATE)**



(4d) Close-up to the fit in (4c) yielding a mean value of  $E = 3259.95(36)$  keV.

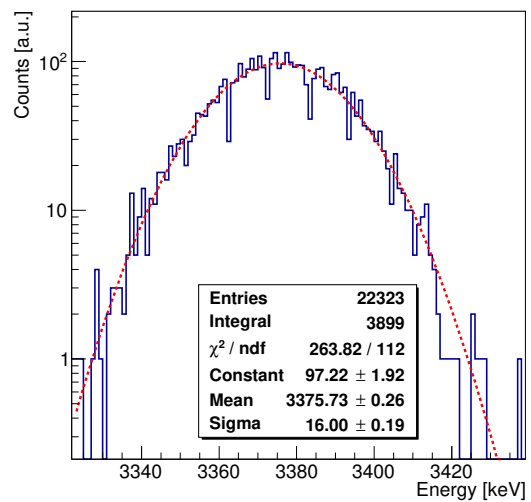
A similar analysis is made taking the data from one of the four silicon detectors on the lower plate, shown in figure 5a, where the ROI in the Fermi energy peak and fitted (Gaussian) presented in 5b. Given a mean energy value of 3375.73(25) keV. In Figure 5c the second case is presented i.e., where the protons go into the opposite direction with respect to the beta particles. Figure ?? shows the close-up to the fit presented in the proton energy yielding a mean value of 3380.18(35) keV, corresponding to a difference in energy of about 4 keV with respect to the singles spectrum.

**Proton Energy Peak (LOWER PLATE)**



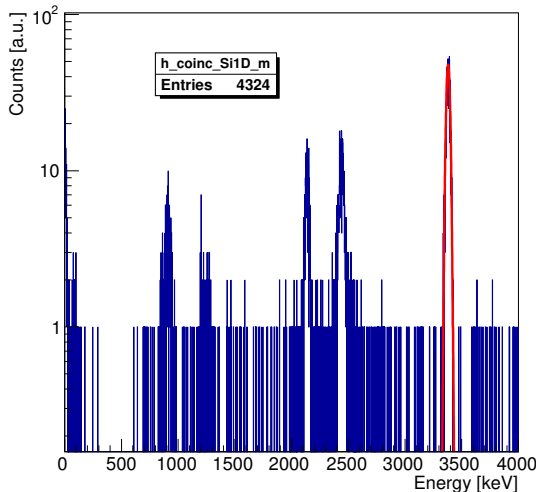
(5a) Proton energy spectrum fitted in the expected ROI (Fermi peak)

**Close-up Proton Energy Peak (LOWER PLATE)**



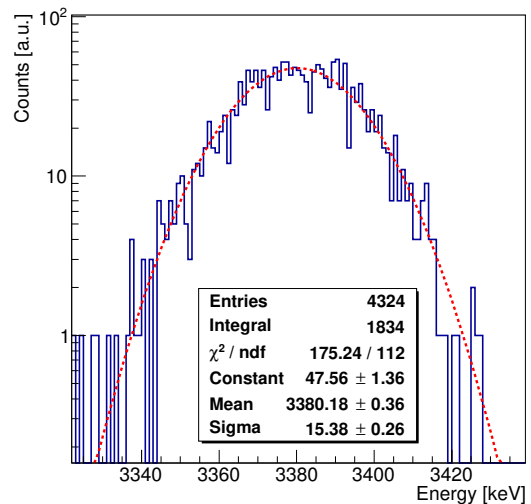
(5b) Close-up to the fit made in (5a) yielding a mean value of  $E = 3375.73(25)$  keV.

**p-beta coincidence (LOWER PLATE)**



(5c) p-beta coincidence energy spectrum fitted in the expected ROI (Fermi peak)

**Close-up p-beta coincidence (LOWER PLATE)**



(5d) Close-up to the fit made in (5c) yielding a mean value of  $E = 3380.18(35)$  keV.

Table 2 summarizes the fitted mean values of a single ROOT file (2 hours of collected data) and the ROI used for each detector.

Table 2: Mean values for each spectrum in the Fermi peak.

case	Silicon 1 UP		Silicon 1 DW	
	ROI [keV]	Mean value	ROI [keV]	Mean value
Single	[3202 - 3316]	3264.92(26)	[3323 - 3438]	3375.73(25)
Coincidence	[3202 - 3316]	3259.95(36)	[3323 - 3438]	3380.18(35)

From the same analysis, it follows that the protons arriving in the Si1UP detector and so going in the same direction as the emitted leptons, also travelled through  $5\mu\text{m}$  thick mylar foil. The implantation profile of  $^{32}\text{Ar}$  ions at 30 keV energy in a mylar foil was computed with SRIM [14] showing that the sample will stop within the first  $1\mu\text{m}$ . The mylar foil used in this first experiment was in the order of  $6\mu\text{m}$  thick generating an energy loss around 100 keV. This difference is seen when comparing the mean energy values for the Si1UP and Si1DW. The second part of the Table 2 shows the mean energy values for the single- and coincidence- histograms for the Silicon 1 DW detector .

## 5. Outlook

Preliminary results show successfully the proof-of-principle of the experiment, since we were able to measure the proton kinematic energy shift, test the functionality of the new control system and optimize the beam injection into the superconducting magnet of the WISArD beamline. Previous MC simulations have shown that the energy resolution of the proton detectors is crucial (less than 10 keV FWHM) to achieve a 0.1% precision of  $a_{\beta\nu}$  measurement. Our proton detectors gave an energy resolution in the order of 40 keV FWHM. Even though the kinematic energy shift is clearly seen, new developments and improvements for the energy resolution in the detection system will be done for new measurements, after the long shutdown at CERN in April 2021. Also, MC simulations are a vital component for understanding the systematic errors present in the experiment, i.e. energy loss due to mylar's thickness and backscattering in the plastic scintillator.

## References

- [1] Allen I S *et al* 1959 *Phys. Rev.* **116** 134
- [2] González-Alonso M and O Naviliat Cuncic 2013 *Ann. Phys. (Berlin)* **525** 600
- [3] Cirigliano V *et al* 2013 *Progr. Part. Nucl. Phys.* **71** 93
- [4] Severijns N and Naviliat-Cuncic O 2013 *Phys. Scripta* **T152** 014018
- [5] González-Alonso M, Naviliat-Cuncic O and Severijns N 2019 *Prog. Part. Nucl. Phys.* **104** 165
- [6] Jackson J D, Treiman S B and Wyld H W 1957 *Phys. Rev.* **106**(3), 517
- [7] Adelberger E *et al* 1999 *Phys. Rev. Lett.* **83** 1299
- [8] Schardt D and Riisager K 1993 *Z. Phys. A* **345** 265
- [9] Blaum K *et al* 2003 *Phys. Rev. Lett.* **91** 26
- [10] Gorelov A *et al* 2005 *Phys. Rev. Lett.* **94** 142501
- [11] Vetter P A *et al* 2008 *Phys. Rev. C* **77**, 035502
- [12] Blank B and Severijns N 2017 *J. Phys. G Nucl. Part. Phys.* **44** 074 002
- [13] Fast Acquisition SysTem for nuclEAR Research *FASTER* LPC-CAEN <http://faster.in2p3.fr>
- [14] Ziegler J F *et al* 2010 *Nucl. Instr. and Meth. Phys. Res. B* **268** 11